HEPATOLOGY

HEPATOLOGY, VOL. 73, NO. 3, 2021

Sirt6 Alleviated Liver Fibrosis by Deacetylating Conserved Lysine 54 on Smad2 in Hepatic Stellate Cells

Jinhang Zhang,[1,2*] Yanping Li,[2*] Qinhui Liu,[2] Ya Huang,[1,2] Rui Li,[1,2] Tong Wu,[1,2] Zijing Zhang,[1,2] Jian Zhou,[1,2] Hui Huang,[1,2] Qin Tang,[1,2] Cuiyuan Huang,[1,2] Yingnan Zhao,[1,2] Guorong Zhang,[1,2] Wei Jiang,[3] Li Mo,[4] Jian Zhang,[5] Wen Xie,[6] and Jinhan He[1,2]

BACKGROUNDS AND AIMS: Activation of hepatic stellate cells (HSCs) is a central driver of fibrosis. This study aimed to elucidate the role of the deacetylase sirtuin 6 (Sirt6) in HSC activation and liver fibrosis.

APPROACH AND RESULTS: Gain-of-function and loss-of-function models were used to study the function of Sirt6 in HSC activation. Mass spectrometry was used to determine the specific acetylation site. The lecithin retinol acyltransferase–driven cyclization recombination recombinase construct (CreERT2) mouse line was created to generate HSC-specific conditional Sirt6-knockout mice ($Sirt6^{\triangle HSC}$). We found that Sirt6 is most abundantly expressed in HSCs as compared with other liver cell types. The expression of Sirt6 was decreased in activated HSCs and fibrotic livers of mice and humans. Sirt6 knockdown and Sirt6 overexpression increased and decreased fibrogenic gene expression, respectively, in HSCs. Mechanistically, Sirt6 inhibited the phosphorylation and nuclear localization of mothers against decapentaplegic homolog (Smad) 2. Further study demonstrated that Sirt6 could directly interact with Smad2, deacetylate Smad2, and decrease the transcription of transforming growth factor β/Smad2 signaling. Mass spectrometry revealed that Sirt6 deacetylated conserved lysine 54 on Smad2. Mutation of lysine 54 to Arginine in Smad2 abolished the regulatory effect of Sirt6. *In vivo*, specific ablation of Sirt6 in HSCs exacerbated hepatocyte injury and cholestasis-induced liver fibrosis in mice. With targeted delivery of the Sirt6 agonist MDL-800, its concentration was 9.28-fold higher in HSCs as compared with other liver cells and alleviated hepatic fibrosis.

CONCLUSIONS: Sirt6 plays a key role in HSC activation and liver fibrosis by deacetylating the profibrogenic transcription factor Smad2. Sirt6 may be a potential therapeutic target for liver fibrosis. (Hepatology 2021;73:1140-1157).

Liver fibrosis is the excessive accumulation of extracellular matrix (ECM) proteins, including collagen. Liver fibrosis can occur in many types of chronic liver diseases that may lead to cirrhosis, liver failure and hepatocellular carcinoma.[1-3] Transdifferentiated (or "activated") hepatic stellate cells (HSCs) represent the major cellular source of ECM-secreting myofibroblasts and the central driver of liver fibrogenesis.[4,5] HSCs exist in the space of Disse and normally are maintained in a quiescent state.[6] When stimulated by external factors, HSCs change from their quiescent state to an activated state, secreting a large amount of ECM and leading to its deposition and causing liver fibrosis.[5]

Transforming growth factor β (TGF-β) is a major profibrogenic cytokine for HSC activation and

Abbreviations: α-SMA, alpha-smooth muscle actin; Ad, adenovirus; aHSC, activated hepatic stellate cell; ALT, alanine aminotransferase; AST, aspartate aminotransferase; CBP, CREB-binding protein; CCl_4, carbon tetrachloride; ChIP, chromatin immunoprecipitation; Col1a1, collagen type I alpha 1 chain; Col1a2, collagen type I alpha 2 chain; Col3a1, collagen type III alpha 1 chain; Cre, cyclization recombination; CreERT2, cyclization recombination recombinase construct; DDC, 5-diethoxycarbonyl-1,4-dihydrocollidine; ECM, extracellular matrix; FBS, fetal bovine serum; HEK293, human embryonic kidney 293; HSC, hepatic stellate cell; Lip, liposome; Lrat, lecithin retinol acyltransferase; Lys, lysine; MS, mass spectrometry; mT/mG, a lineage-tracking mouse line; PAGE, polyacrylamide gel electrophoresis; qHSC, quiescent hepatic stellate cell; SDS, sodium dodecyl sulfate; Sirt6, sirtuin 6; $Sirt6^{f/f}$, Sirt6 floxed mice; $Sirt6^{\triangle HSC}$, HSC-specific conditional Sirt6-knockout mice; Smad, mothers against decapentaplegic homolog; Ser, serine; TGF-β, transforming growth factor β; Tris, trishydroxymethylaminomethane; WT, wild type.

Received January 29, 2020; accepted May 20, 2020.

Additional Supporting Information may be found at onlinelibrary.wiley.com/doi/10.1002/hep.31418/suppinfo.

Supported by the National Natural Science Foundation of China (81930020, 81873662, and 81870599), research funding from Sichuan Province (2018SZ0158), and Post-Doctor Research Project, West China Hospital of Sichuan University (2018HXBH060). The authors thank Huifang Li, Yan Wang, and Zhen Yang from Core Facility of West China Hospital and Li Li and Fei Chen from the Laboratory of Pathology, West China Hospital for technical assistance.

**These authors contributed equally to this work.*

induction of the fibrotic response.[7,8] TGF-β binds to its receptor and leads to the phosphorylation of mothers against decapentaplegic homolog (Smad) 2 and Smad3. The phosphorylation of Smad2/3 is required for their nuclear translocation and transcriptional regulation of their fibrotic target genes.[9] Recent studies suggested that acetylation of Smad2 may affect its transcriptional activity. For instance, it has been reported that p300/CREB-binding protein (CBP) can acetylate Smad2 and enhance its ability to mediate TGF-β signaling.[10] Acetylation of Lysine(Lys)19 on Smad2 induced a conformational change in the MH1 domain, so its DNA binding domain was accessible for interacting with DNA.[11] Acetylation is reversible, but which deacetylase is responsible for the deacetylation of Smad2 and whether the Smad2 deacetylase plays a role in HSC activation and liver fibrosis remain unclear.

Sirtuin 6 (Sirt6) is a member of the sirtuin family of NAD^+-dependent deacetylases, with diverse roles in aging, metabolism and disease.[12] Sirt6 whole-body knockout mice have a shortened lifespan and phenotypes associated with aging, cancer, and metabolic disorders.[12-15] Such mice also showed the progression of chronic liver inflammation and fibrosis.[12-16] By using hepatocyte-specific Sirt6-knockout mice, Ka and colleagues showed that the observed liver fibrosis may be a secondary effect due to injury to hepatocytes.[17] In Sirt6 whole-body knockout mice, TGF-β signaling was up-regulated and led to collagen deposition and ECM remodeling.[16] In humans, the expression of Sirt6 was significantly lower in fibrotic livers than healthy livers.[17] These studies suggest that Sirt6 may play an important role in regulating hepatic fibrosis. However, the direct role of Sirt6 in HSC activation and liver fibrosis remains unknown.

In the present study, we found that Sirt6 is most highly expressed in HSC among all liver cell types. Sirt6 expression was decreased in activated HSCs (aHSCs) and fibrotic livers. Sirt6 played an important role in preventing HSC activation by inhibiting TGF-β signaling. Sirt6 physically interacted with Smad2, deacetylated the conserved lysine 54 residue, and regulated Smad2 transcriptional activity. The lecithin retinol acyltransferase (Lrat)-CreERT2 mouse line was created to specifically delete Sirt6 in HSCs. HSC-specific deletion of Sirt6 exacerbated mouse models of liver fibrosis. Conversely, pharmacological activation of Sirt6 protected mice against liver fibrosis. Our results suggest that Sirt6 may be a promising therapeutic target for liver fibrosis.

Materials and Methods

ANIMAL EXPERIMENTS

Animal protocols were approved by Sichuan University Animal Care and Use Committee. Floxed

View this article online at wileyonlinelibrary.com.
DOI 10.1002/hep.31418

Potential conflict of interest: Nothing to report.

ARTICLE INFORMATION:

From the [1]Department of Pharmacy, State Key Laboratory of Biotherapy, West China Hospital, Sichuan University, Chengdu, China; [2]Laboratory of Clinical Pharmacy and Adverse Drug Reaction, West China Hospital, Sichuan University, Chengdu, China; [3]Molecular Medicine Research Center, West China Hospital of Sichuan University, Chengdu, China; [4]Center of Gerontology and Geriatrics West, China Hospital of Sichuan University, Chengdu, China; [5]Department of Pathophysiology, Key Laboratory of Cell Differentiation and Apoptosis of Chinese Ministry of Education, Shanghai Jiao-Tong University School of Medicine (SJTU-SM), Shanghai, China; [6]Center for Pharmacogenetics and Department of Pharmaceutical Sciences, University of Pittsburgh, Pittsburgh, PA.

ADDRESS CORRESPONDENCE AND REPRINT REQUESTS TO:

Jinhan He, Ph.D.
Department of Pharmacy, State Key Laboratory of Biotherapy and Cancer Center, West China Hospital of Sichuan University and Collaborative Innovation Center of Biotherapy
No. 37 Guoxue Lane, Wuhou District, Chengdu 610041 Sichuan, China
E-mail: jinhanhe@scu.edu.cn
Tel.: +1-86-28-85426416

$Sirt6^{f/f}$ and mT/mG mice, a lineage-tracking mouse line, were purchased from the Jackson Laboratory (Bar Harbor, ME). Lrat-CreERT2 knock-in mice were created by integrating an inducible cyclization recombination (Cre) recombinase construct (*CreERT2*) in the 3′ untranslated region of the endogenous mouse *Lrat* gene. Lrat-CreERT2 mice were crossed with $Sirt6^{f/f}$ mice to generate HSC-specific conditional Sirt6-knockout mice ($Sirt6^{\triangle HSC}$). Lrat-CreERT2 mice were also bred with mT/mG mice to track the expression of CreERT2 recombinase. To induce the recombination, mice were injected with tamoxifen (100 mg/kg) every other day 5 times. C57BL/6J mice were injected with Carbon tetrachloride (CCl_4) (0.75 mL/kg, Sigma-Aldrich, St. Louis, MO) twice a week for 8 weeks to induce liver fibrosis. In another model, C57BL/6J mice were fed a standard (control) diet or the standard diet supplemented with 0.1% 5-diethoxycarbonyl-1,4-dihydrocollidine (DDC; Sigma-Aldrich, Vienna, Austria) for 4 weeks.

CELL LINE TREATMENT

The human HSC line LX-2 was provided by Lieming Xu from Shuguang Hospital, Shanghai University of Traditional Chinese Medicine. LX-2 cells and human embryonic kidney 293 (HEK293) cells were cultured in Dulbecco's modified Eagle's medium (DMEM; Gibco) supplemented with 10% fetal bovine serum (FBS; Hyclone) and incubated at 37℃ with 5% CO_2.

ISOLATION AND CULTURE OF PRIMARY HSCs

Mouse HSCs were isolated by collagenase digestion followed by centrifugation in an OptiPrep gradient, as described,[18] and then cultured in DMEM containing 10% FBS overnight, and the medium was changed every 2 days.

LUCIFERASE ASSAY

HEK293 cells were seeded in 48-well plates and transiently cotransfected with Smad binding element (SBE) luciferase reporter and Smad2 with or without Sirt6. After 48 hours of transfection, HEK293 cells were stimulated with TGF-β1 (2 ng/mL) for 1 hour, and cells were harvested to detect luciferase. β-galactosidase activity was used to normalize transfection efficiency.

COIMMUNOPRECIPITATION

Nuclear extracts were prepared from HEK293 cells by using a cytoplasmic and nuclear protein isolation kit (Beyotime, P0028). For coimmunoprecipitation, cells were lysed with nondenaturing Nonidet P40 lysis buffer (50 mM trishydroxymethylaminomethane [Tris], pH 7.5, 150 mM sodium chloride, 1 mM ethylene diamine tetraacetic acid, 0.25% sodium deoxycholate) supplemented with 1 mM phenylmethylsulfonyl fluoride, protease inhibitor cocktail, and phosphatase inhibitor cocktail (Sigma). An amount of 500 μg protein was immunoprecipitated with anti-Sirt6 or anti-total-Smad2/3 antibody and Protein A/G PLUS-Agarose (sc-2003, Santa Cruz Biotechnology) overnight at 4°C. Beads with the immune-precipitated complex were washed with lysis buffer three times before denaturing in lysis buffer (0.1M Tris-hydrochloric acid [HCl] pH 6.8, 4% SDS, 20% glycerol, sodium pyrophosphate, 1 mM sodium orthovanadate [Na3VO4], sodium fluoride [NaF]) at 97°C for 10 minutes. Nuclear extracts and immunoprecipitated protein were resolved by SDS-PAGE.

CHROMATIN IMMUNOPRECIPITATION

LX-2 cells were infected with adenovirus (Ad)-Sirt6 for 48 hours and then treated with TGF-β1 (2 ng/mL) for 4 hours. The next steps were performed with the EZ-Magna Chromatin Immunoprecipitation (ChIP) G Kit (Millipore, Billerica, MA). Purified DNA was subjected to RT-PCR.

MASS SPECTROMETRY IDENTIFICATION OF ACETYLATION SITES

HEK293 cells were transfected with Smad2 with or without Sirt6 and then 48 hours later were treated with TGF-β1, and the nuclear fraction was prepared by using a kit (Beyotime, P0028). The nuclear protein was immunoprecipitated with antiacetylation antibody and Protein A/G PLUS-agarose (sc-2003, Santa Cruz Biotechnology) overnight at 4°C. Immunoprecipitated protein was resolved by 10% SDS-PAGE gels for Coomassie blue staining. The gels were used for mass spectrometry (MS).

IMMUNOFLUORESCENCE STAINING

Samples of cells and liver sections were fixed in 4% paraformaldehyde for 10 minutes, then incubated in 0.2% Triton X-100 1× phosphate-buffered saline for 15 minutes for permeabilization of the cytomembrane. Cell and tissue samples were incubated with primary antibodies at 4°C overnight. All antibodies used are in Supporting Table S1.

HYDROXYPROLINE ASSAY

Total collagen content was tested by measuring the amount of hydroxyproline in liver tissue by using commercially available hydroxyproline detection kits (Nan Jing Jan Cheng Biochemical Institute, Nanjing, China) according to the manufacturer's instructions.

HISTOLOGY

Livers were fixed in 10% formalin, embedded in paraffin, sectioned at 4 μm, and stained with hematoxylin and eosin, Sirius red, and Masson to examine the extent of inflammation and liver fibrosis. Images were captured under a microscope (Nikon, Tokyo).

WESTERN BLOT ANALYSIS

Cells and tissues were lysed in lysis buffer (0.1 M Tris-HCl pH 6.8, 4% SDS, 20% glycerol, sodium pyrophosphate, 1 mM Na3VO4, NaF) and applied to 10% SDS-PAGE gels and probed with antibodies. Blots were visualized by using the LI-COR Odyssey System (Lincoln, NE). Quantitative determination of band intensity involved using Image Studio v4.0 (LI-COR). Antibodies are listed in Supporting Table S1.

QUANTITATIVE REAL-TIME PCR

Total RNA extracted from liver or cells by using Trizol reagent (Applygen, Beijing, China) and reverse-transcribed into complementary DNA (RR037A; TaKaRa, Kyoto, Japan). Quantitative real-time PCR involved the SYBR green-based assay with the CFX96 Real-Time system (Bio-Rad, Hercules, CA). The sequences of primers for real-time PCR are in Supporting Table S2.

STATISTICS

All quantitative data are expressed as mean ± SEM. All studies were repeated at least three times with similar results. Student *t* test was used to compare two groups. One-way ANOVA followed by the Dunnett post-hoc test was used for multiple comparisons (GraphPad Software). $P < 0.05$ was considered statistically significant.

Results

Sirt6 IS HIGHLY EXPRESSED IN HSCs, AND THE EXPRESSION OF Sirt6 IS DECREASED IN aHSCs AND FIBROTIC LIVER

To explore the potential role of Sirt6 in liver fibrosis, we first compared the expression of Sirt6 in different types of cells isolated from the liver. Surprisingly, among the cell types evaluated, HSCs had the most abundant expression of Sirt6 (Supporting Fig. S1A). Freshly isolated HSCs were considered quiescent HSCs (qHSCs), and when cultured for 7 days, qHSCs become aHSCs.[18] With the onset of HSC activation, the protein expression of Sirt6 was greatly decreased (Fig. 1A, left and right panels). In mouse models of liver fibrosis induced by CCl_4 or DDC, the expression of Sirt6 was also markedly decreased (Fig. 1B, left panel, and Fig. 1C, left panel). With the colocalization of Sirt6 and desmin, the expression of Sirt6 was reduced in HSCs (Fig. 1B, right panel, and Fig. 1C, right panel). Similarly, we found the expression of Sirt6 in HSCs isolated from fibrotic livers was also decreased (Supporting Fig. S1C,D, left panels). The purity of isolated HSC was estimated to be higher than 95% (Supporting Fig. S1C,D, right panels). The validation of the Sirt6 antibody is shown in Supporting Fig. S1E,F. Aging is known to be a major risk factor for the development of liver fibrosis in healthy individuals. Isolated HSCs from old mice (12 months old) showed lower expressions of Sirt6 compared with young mice (3 months old) (Supporting Fig. S1B). Also, the hepatic expression of Sirt6 in HSC was decreased in patients with liver fibrosis (Fig. 1D). Taken together, these results suggest that Sirt6 may play a role in HSC activation and liver fibrosis.

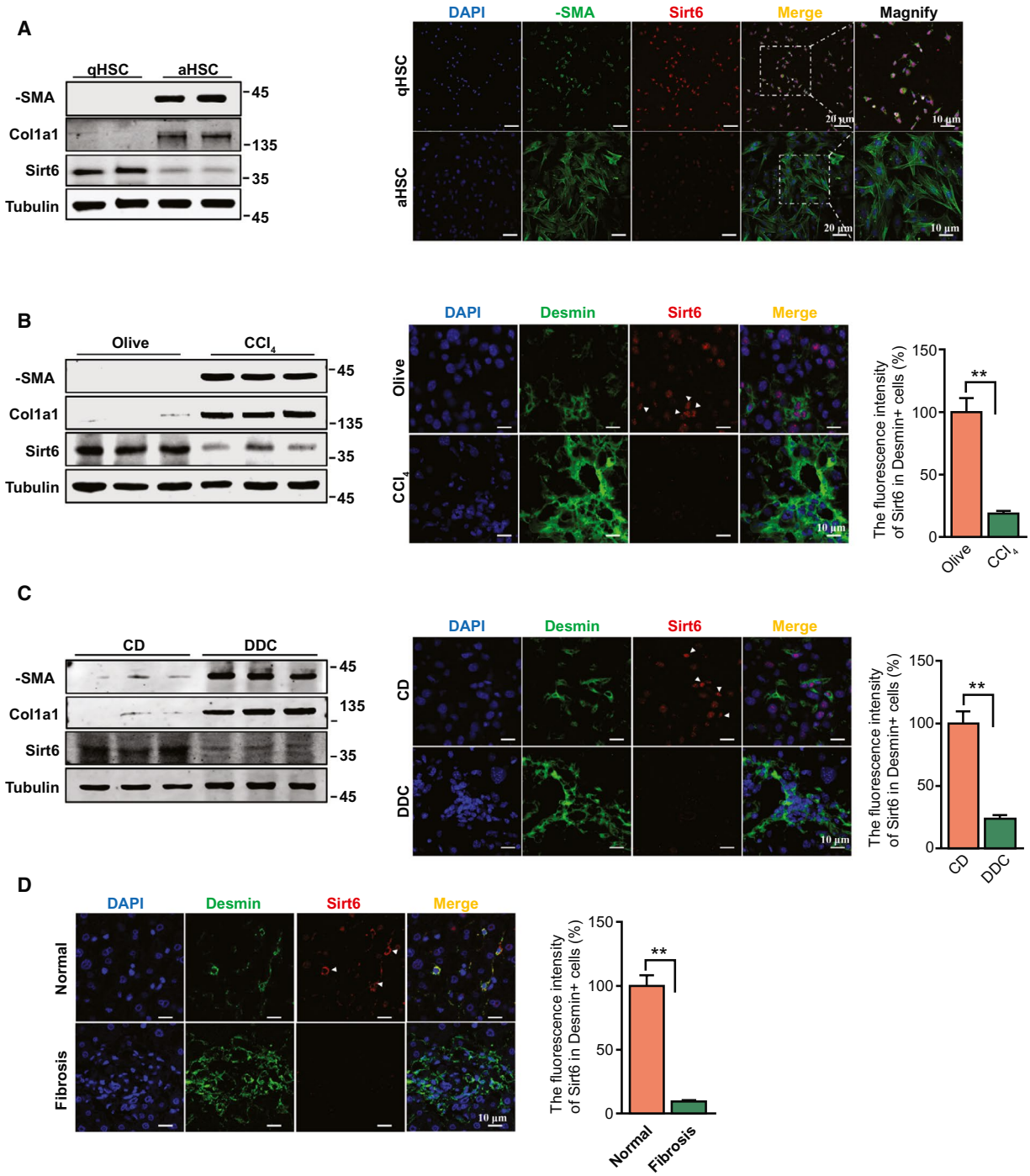

FIG. 1. The expression of Sirt6 was decreased in aHSCs and fibrotic livers of mice and humans. (A) Sirt6 expression was decreased by HSC activation. Primary HSCs were isolated from WT mice and cultured for 1 day (qHSCs) or 7 days (aHSCs). Left panel: western blot analysis of α-SMA, Col1a1, and Sirt6 expression. Right panel: immunofluorescent staining of α-SMA accumulation and Sirt6 expression in qHSCs and aHSCs. (B) Sirt6 expression was decreased in the fibrotic liver of CCl_4-treated mice. WT mice were injected with CCl_4 or vehicle for 8 weeks. Sirt6 expression were detected by western blot analysis, immunofluorescence staining, and quantification of Sirt6 fluorescent signal. (C) Sirt6 expression was decreased in fibrotic liver of mice induced by DDC. WT mice were fed with or without a 0.1% DDC diet for 4 weeks. Sirt6 expression were detected by western blot analysis, immunofluorescence staining, and quantification of Sirt6 fluorescent signal. (D) Liver sections were collected from normal individuals or patients with liver fibrosis and stained with Sirt6 and desmin. Right panel: quantification of Sirt6 fluorescent signal. Data are mean ± SEM. $^*P < 0.05$, $^{**}P < 0.01$. Abbreviation: DAPI, 4′,6-diamidino-2-phenylindole.

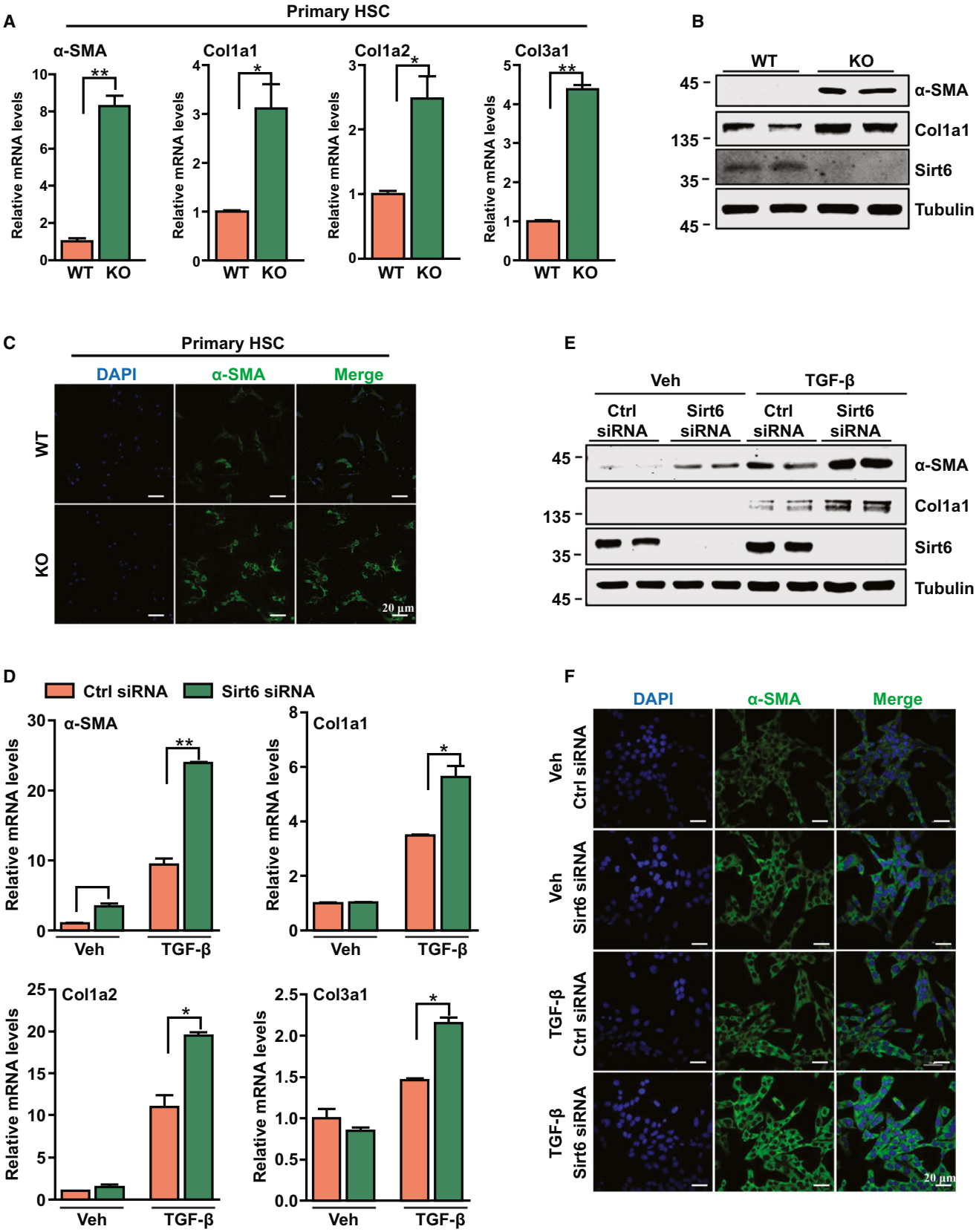
A
Primary HSC
α-SMA
Col1a1
Col1a2
Col3a1
Relative mRNA levels
WT KO
B
WT KO
45
135
35
45
α-SMA
Col1a1
Sirt6
Tubulin
C
Primary HSC
DAPI
α-SMA
Merge
WT
KO
20 μm
E
Veh
TGF-β
Ctrl siRNA
Sirt6 siRNA
45
135
35
45
α-SMA
Col1a1
Sirt6
Tubulin
D
Ctrl siRNA
Sirt6 siRNA
α-SMA
Col1a1
Col1a2
Col3a1
Relative mRNA levels
Veh
TGF-β
F
DAPI
α-SMA
Merge
Veh Ctrl siRNA
Veh Sirt6 siRNA
TGF-β Ctrl siRNA
TGF-β Sirt6 siRNA
20 μm

FIG. 2. Knockdown of Sirt6 promoted TGF-β–induced HSC activation. (A-C) Mouse primary HSCs were isolated from Sirt6$^{f/f}$ mice, cultured for 2 days, and then infected with Ad-green fluorescent protein or Ad-Cre to knock down Sirt6 for 48 hours. (A) Real-time quantitative PCR analysis of the mRNA expression of fibrotic genes. (B) Western blot analysis of the protein expression of α-SMA, Col1a1, and Sirt6. (C) Immunofluorescence staining of α-SMA. (D-F) Human LX-2 cells were transfected with Sirt6 small interfering RNA (siRNA) to knock down Sirt6 expression under 2% FBS condition and then treated with TGF-β (2 ng/mL). (D) Real-time quantitative PCR analysis of the mRNA expression of fibrotic genes. (E) Western blot analysis of the protein expression of α-SMA, Col1a1, and Sirt6. (F) Immunofluorescence staining of α-SMA expression. Data are mean ± SEM. n = 3 experiments, each in triplicate. $^{*}P < 0.05$, $^{**}P < 0.01$. Abbreviations: Ctrl, control; DAPI, 4′,6-diamidino-2-phenylindole; KO, knockout; Veh, vehicle.

KNOCKDOWN OF Sirt6 SENSITIZES HSCs TO ACTIVATION

To directly evaluate the role of Sirt6 in HSC activation, we isolated primary HSCs from Sirt6$^{f/f}$ mice and infected them with Ad-Cre to knock down Sirt6 expression. The adenoviral infection efficiency was estimated to be more than 98% (Supporting Fig. S2A). Knockdown of Sirt6 increased the activation-responsive mRNA expression of fibrotic genes such as alpha-smooth muscle actin (*α-SMA*), collagen type I alpha 1 chain (*Col1a1*), collagen type I alpha 2 chain (*Col1a2*), and collagen type III alpha 1 chain (*Col3a1*) (Fig. 2A). Western blot analysis confirmed the elevated protein expression of α-SMA and Col1a1 when Sirt6 was knocked down (Fig. 2B). Immunofluorescent staining revealed α-SMA signal more detectable in Sirt6 knockdown HSCs than other cells (Fig. 2C). In LX-2 cells, a human HSC cell line, Sirt6 knockdown, enhanced the TGF-β-stimulated mRNA expression of the fibrotic genes *α-SMA*, *COL1A1*, *COL1A2*, and *COL3A1* (Fig. 2D). The increased protein expression of α-SMA and/or COL1A1 in TGF-β–treated LX-2 cells with Sirt6 knockdown was verified by western blot analysis (Fig. 2E) and immunofluorescent staining (Fig. 2F).

OVEREXPRESSION OR PHARMACOLOGICAL ACTIVATION OF Sirt6 INHIBITS HSC ACTIVATION

The loss-of-function study prompted us to determine whether overexpression of Sirt6 could inhibit the activation of HSCs. In culture-activated primary HSCs, Sirt6 overexpression greatly reduced the mRNA expression of fibrotic genes such as *α-SMA*, *Col1a1*, *Col1a2*, and *Col3a1* (Fig. 3A and Supporting Fig. S2B). The decreased protein expression of α-SMA and Col1a1 was confirmed by western blot analysis (Fig. 3B). Immunostaining also showed the lower expression of α-SMA (Fig. 3C). Overexpression of Sirt6 also inhibited TGF-β–induced activation of LX-2 cells (Fig. 3D-F).

We next determine whether pharmacological activation of Sirt6 would have a similar effect on inhibiting the activation of HSCs. ML-800 is a selective agonist of Sirt6.[19] In this experiment, we used an HSC-specific drug delivery system by modifying sterically stable liposome (Lip) with Cyclo [Arg-Gly-Asp-DTyr-Lys] (cRGDyK), RGD-Lip, a pentapeptide that binds to aHSCs.[20] We loaded RGD-Lip with MDL-800 to produce RGD-Lip/MDL-800. The schematic illustration, particle size, morphology, and entrapment efficiency of the RGD-Lip delivery system are in Supporting Fig. S3A-D. The specificity of the drug delivery system was confirmed by the uptake of RGD-Lip loaded with the fluorescent dye DiD in different types of cells isolated from the liver (Supporting Fig. S3E,F). RGD-Lip/MDL-800 significantly suppressed the expression of fibrotic genes including, *α-SMA*, *Col1a1*, *Col1a2*, and *Col3a1*, in primary HSCs (Supporting Fig. S4A-C). In LX-2 cells, RGD-Lip/MDL-800 had a similar inhibitory effect on the activation of LX-2 cells induced by TGF-β (Supporting Fig. S4D,E). All these results suggest that Sirt6 plays an inhibitory role in HSC activation.

Sirt6 INHIBITED HSC ACTIVATION BY INHIBITING TGF-β SIGNALING

TGF-β plays a key role in HSC activation and fibrosis by including the phosphorylation and nuclear translocation of Smad2/3.[21] To understand the mechanism by which Sirt6 inhibits fibrogenesis, we first measured the TGF-β signaling pathway. Sirt6 overexpression could significantly inhibit the phosphorylation of Smad2 induced by TGF-β (Fig. 4A). The phosphorylation of Smad2 leads to translocation from cytoplasm to nucleus.[22] Sir6

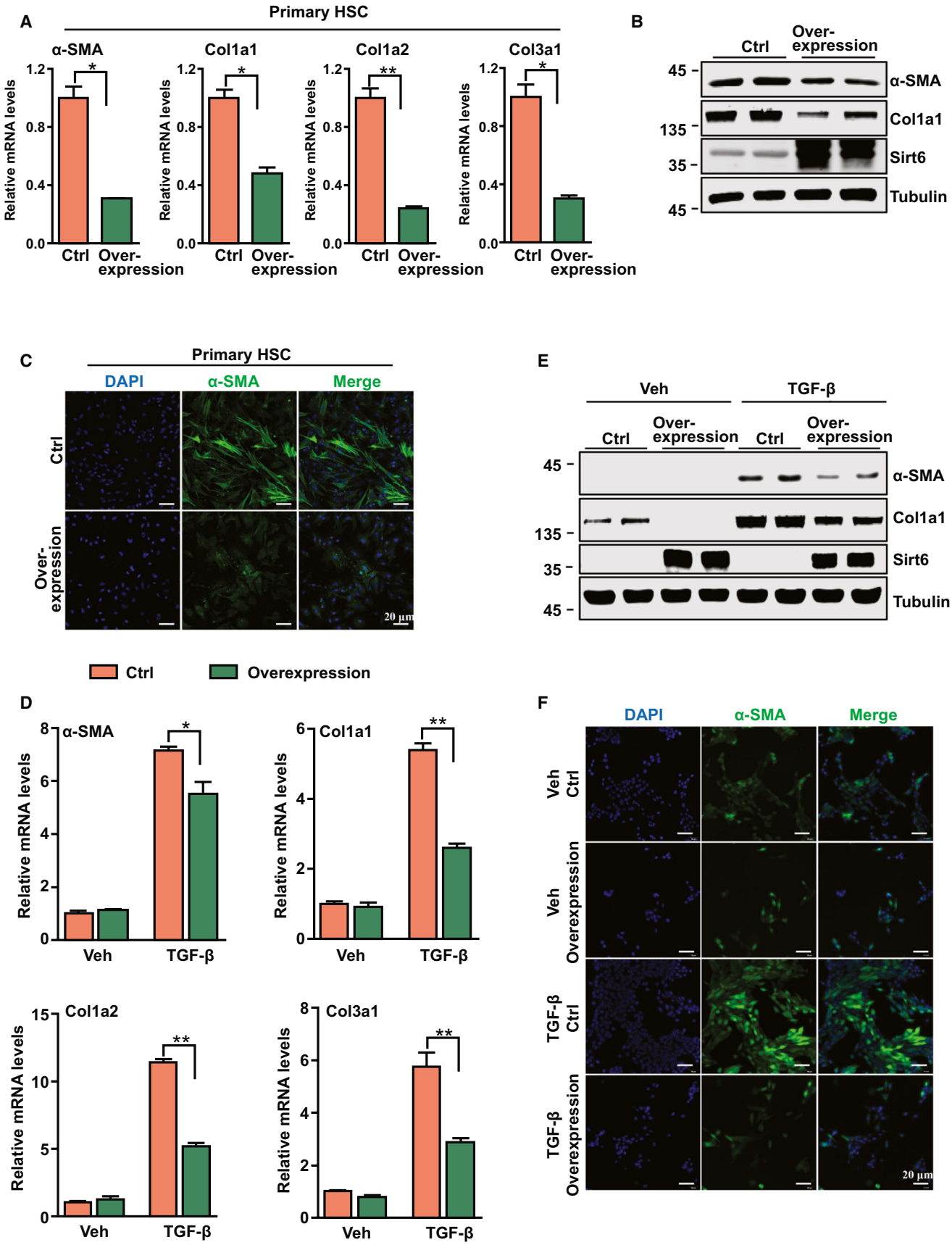
A
Primary HSC
α-SMA
Col1a1
Col1a2
Col3a1
Relative mRNA levels
Ctrl
Over-expression
B
Ctrl
Over-expression
45
135
35
45
α-SMA
Col1a1
Sirt6
Tubulin
C
Primary HSC
DAPI
α-SMA
Merge
Ctrl
Over-expression
20 μm
Ctrl
Overexpression
D
α-SMA
Col1a1
Col1a2
Col3a1
Relative mRNA levels
Veh
TGF-β
E
Veh
TGF-β
Ctrl
Over-expression
45
135
35
45
α-SMA
Col1a1
Sirt6
Tubulin
F
DAPI
α-SMA
Merge
Veh Ctrl
Veh Overexpression
TGF-β Ctrl
TGF-β Overexpression
20 μm

FIG. 3. Overexpression of Sirt6-ameliorated TGF-β–induced HSC activation. (A-C) Mouse primary HSCs were isolated from WT mice and cultured for 7 days under 10% FBS condition and then infected with Ad-Sirt6 to overexpress Sirt6. (A) Real-time quantitative PCR analysis of the mRNA expression of fibrotic genes. (B) Western blot analysis of the protein expression of α-SMA, Col1a1, and Sirt6. (C) Immunofluorescence analysis of α-SMA expression. (D,E) Human LX-2 cells were infected with Ad-green fluorescent protein or Ad-Sirt6 under 2% FBS condition and then treated with TGF-β (2 ng/mL) for 48 hours. (D) Real-time quantitative PCR analysis of the mRNA expression of fibrotic genes. (E) Western blot analysis of the protein levels of α-SMA and Col1a1. (F) Immunofluorescence staining of α-SMA expression. Data are mean ± SEM. n = 3 experiments, each in triplicate. $^{*}P < 0.05$, $^{**}P < 0.01$. Abbreviations: Ctrl, control; DAPI, 4′,6-diamidino-2-phenylindole; Veh, vehicle.

overexpression significantly inhibited the TGF-β–induced Smad2 translocation from cytoplasm to nucleus (Fig. 4B-C). Coimmunoprecipitation showed that Sirt6 could interact with Smad2, which was further enhanced by TGF-β stimulation (Fig. 4D, upper left and right panels). We determined whether Smad2 is the direct substrate for the deacetylase activity of Sirt6 by deacetylation assay in HEK293 cells. TGF-β treatment increased the acetylation of Smad2, which was abolished by the overexpression of Sirt6 (Fig. 4D, lower left and right panels). Luciferase reporter assay further showed that cotransfection of Sirt6 decreased the transcriptional activity of Smad2 (Fig. 4E). Finally, ChIP assay demonstrated that Sirt6 reduced the recruitment of Smad2 to promoter regions of *Col1a1* and *Col1a2* genes (Fig. 4F). Together, these results suggest that Sirt6 could deacetylate Smad2 and regulate its transcriptional activity.

Sirt6 DEACETYLATES Smad2 ON K54

To map the deacetylation site of Smad2 by Sirt6, we used MS of Smad2-overexpressing HEK293 cells with or without Sirt6. Lysine 54 of Smad2 was the only amino acid found deacetylated by Sirt6 (Fig. 5A, left panel). Lysine 54 in Smad2 is highly conserved among different species from *Mnemiopsis leidyi* to *Homo sapiens* (Fig. 5A, right panel), which indicates an important role of K54 in Smad2. The mutation of lysine to Arginine at this position decreased the acetylation level of Smad2 and abolished the regulatory effect of Sirt6 (Fig. 5B, left and right panels). At the functional level, mutation of lysine 54 decreased TGF-β–induced phosphorylation of Smad2 (Fig. 5C, upper panel). The nuclear-localized Smad2 was consistently decreased by mutation of lysine 54 (Fig. 5C, lower panel). Immunofluorescence staining exhibited reduced nuclear accumulation of Smad2 when lysine 54 was mutated (Fig. 5D, left panel). Luciferase assay showed the lower transcriptional activity of mutant Smad2 (Fig. 5D, right panel). Lysine 54 appeared to be required for the effects of Sirt6 on cellular localization and transcriptional activity of Smad2 because mutation of lysine 54 abolished the effect of Sirt6 on decreasing the phosphorylation and nuclear localization of Smad2 (Fig. 5E, upper panel and lower panel, and Fig. 5F, left panel) and transcriptional activity of Smad2 (Fig. 5F, right panel). Together, Sirt6 may regulate the deacetylation of lysine 54 on Smad2, playing an important role in Smad2 phosphorylation, nuclear translocation, and transcriptional activity.

GENERATION OF HSC-SPECIFIC Sirt6-KNOCKOUT MICE

To explore the HSC-specific function of Sirt6 in liver fibrosis *in vivo*, we created a tamoxifen-inducible Lrat-driven CreERT2 mouse line. Lrat is known as an HSC-specific gene.[23] We also found that Lrat is expressed in HSCs but not in other liver cell types (Supporting Fig. S5A). *CreERT2* was knocked into the downstream of *Lrat* connected by 2A (Lrat-CreERT2) (Fig. 6A). To track the expression of CreERT2 recombinase, Lrat-CreERT2 mice were bred with mT/mG mice, a lineage-tracking mouse line. In tamoxifen-treated normal mice, the expression of Cre overlapped with the fluorescent signal of α-SMA (Supporting Fig. S5B). In tamoxifen-treated fibrotic mice induced with CCl_4, the expression of Cre was strong and was confined to α-SMA–positive HSCs (Supporting Fig. S5B). The expression of Cre was barely detectable in cells positive for hepatocyte nuclear factor 1β, CD31, Cytokeratin 19 (CK19), and F4/80, which are markers of hepatocytes, biliary cells, endothelia cells, and Kupffer cells, respectively

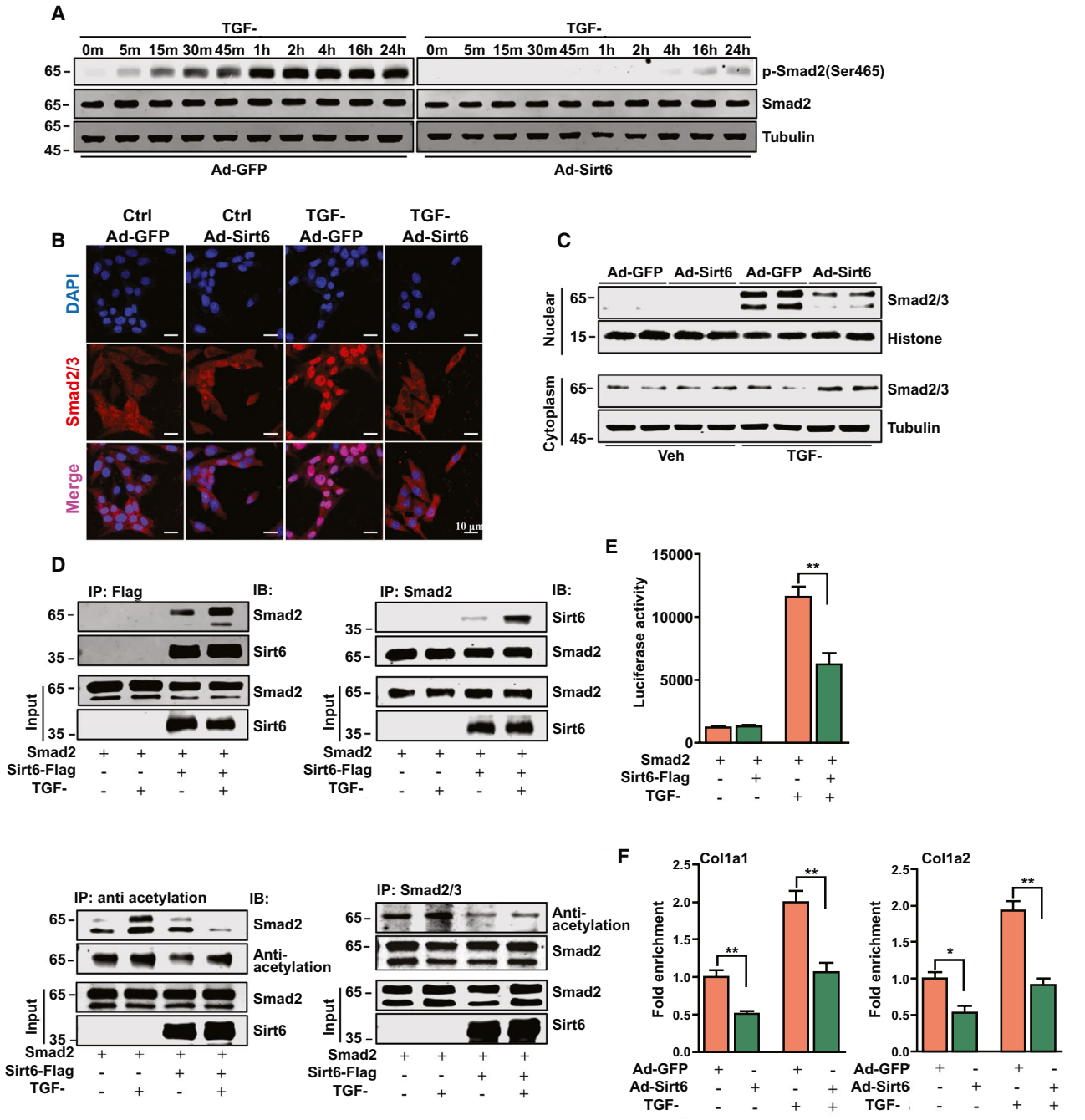

FIG. 4. Sirt6 inhibited HSC activation by modulating the TGF-β signaling pathway. (A-C) LX-2 cells were infected with Ad-green fluorescent protein (GFP) or Ad-Sirt6 and then treated with or without TGF-β (2 ng/mL) for the indicated time. (A) Western blot analysis of the protein expression of phosphorylated (p-)Smad2 and Smad2. (B) Immunofluorescent staining of cellular Smad2 and (C) nuclear and cytoplasm fraction of Smad2. (D) HEK293 cells were transfected with Smad2 and then treated with or without TGF-β1 (2 ng/mL). Upper left and right panel: whole cell lysates were immunoprecipitated with anti-Sirt6 or anti-Smad2 antibodies, and precipitated proteins were detected by anti-Smad2 or anti-Sirt6 antibodies. Lower left and right panel: western blot detection of nuclear acetylation levels of Smad2 in HEK293 cells with or without TGF-β treatment. (E) HEK293 cells were transfected with the Smad reporter (SBE reporter) and Smad2 with or without Sirt6 and then treated with or without TGF-β1 for 18 hours. Luciferase activity was normalized to β-galactosidase. (F) ChIP assay of LX-2 cells infected with Ad-GFP or Ad-Sirt6, then treated with or without TGF-β. Data are mean ± SEM. n = 3 experiments, each in quadruplicate. $^{*}P < 0.05$, $^{**}P < 0.01$. Abbreviations: Ctrl, control; DAPI, 4′,6-diamidino-2-phenylindole; IB, immunoblotting; IP, immunoprecipitation; Veh, vehicle.

(Supporting Fig. S5C-F). Lrat-CreERT2 mice were bred with Sirt6$^{f/f}$ mice to generate Sirt6$^{\triangle HSC}$ (Fig. 6A). On tamoxifen treatment, Sirt6 was specifically knocked out in HSCs but not in other liver cell types of Sirt6$^{\triangle HSC}$ mice (Fig. 6B, upper panel, and Supporting Fig. S6A-C). The endogenous expression of Lrat was not affected by tamoxifen or Sirt6 deletion (Fig. 6B, upper panel). These results demonstrated successful creation of an HSC-specific Sirt6 knockout mouse line.

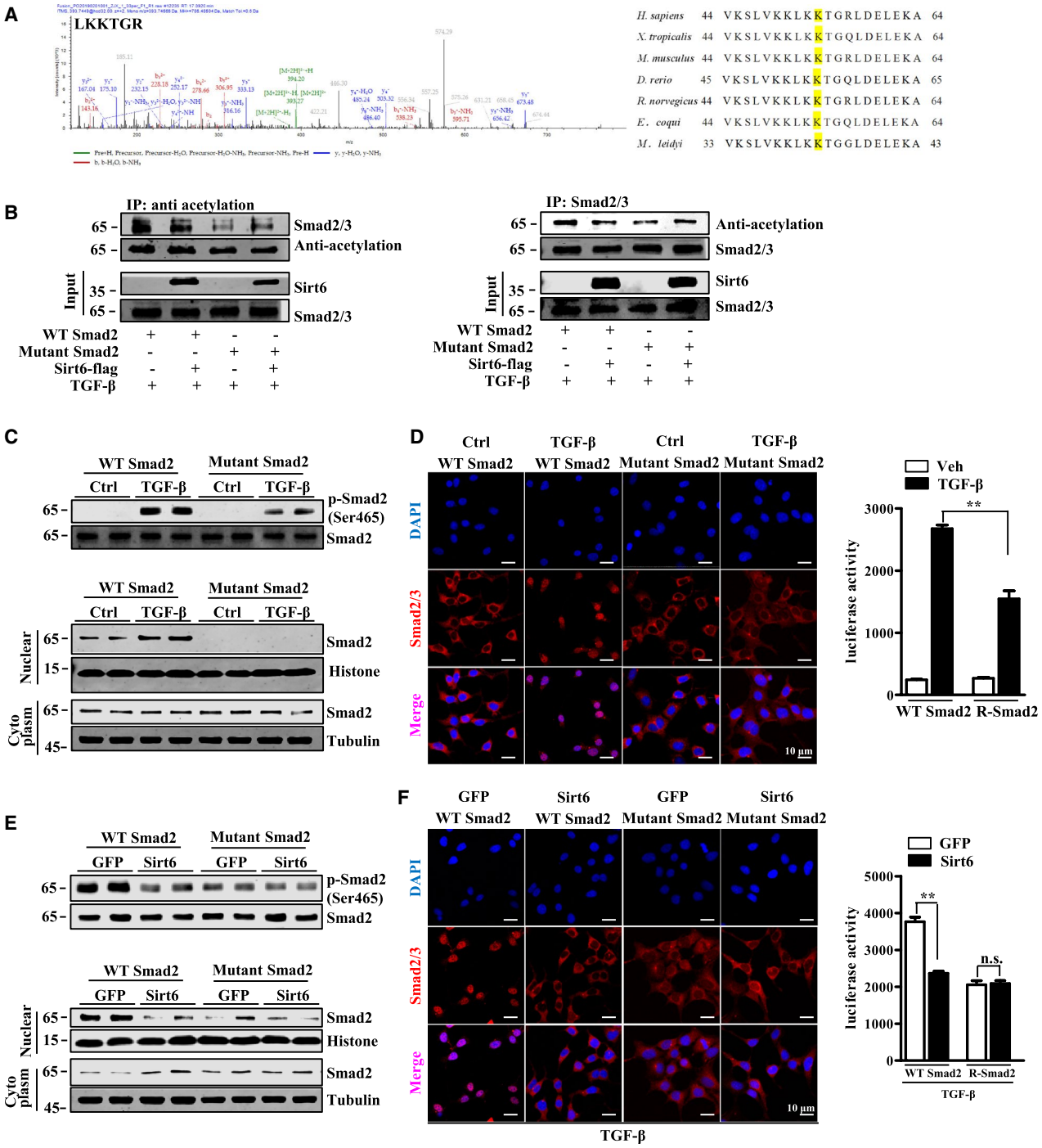

FIG. 5. Sirt6 regulated TGF-β signaling by deacetylating lysine 54 on Smad2. (A) MS identified Sirt6 deacetylated lysine 54 in Smad2. Lysates from HEK293 cells with or without Sirt6 treatment were resolved by SDS-PAGE. Right panel: conservation of Smad2 lysine 54 in different species. (B) Sirt6 deacetylated Smad2 through lysine 54. Lysine 54 in Smad2 was mutated to alanine. Western blot analysis of acetylation level of WT Smad2 with Sirt6 treatment. (C,D) Role of Smad2 deacetylation at lysine 54 in TGF-β signaling. HEK293 cells were transfected with WT Smad2 or mutant Smad2, followed by TGF-β treatment. (C) Upper panel: the phosphorylation of Smad2. Lower panel: the cellular localization of Smad2. (D) Left panel: immunofluorescent staining of Smad2. Right panel: transcriptional activity of WT and mutant Smad2. HEK293 cells were cotransfected with WT Smad2 or mutant Smad2, followed by Sirt6 treatment. (E,F) Lysine 54 on Smad2 is required for Sirt6-regulated TGF-β signaling pathway. (E) Upper panel: phosphorylation of Smad2. Lower panel: cellular localization of Smad2. (F) Left panel: immunofluorescent staining of Smad2. Right panel: transcriptional activity of WT and mutant Smad2. Data are mean ± SEM. n = 3 experiments, each in quadruplicate. $^{**}P < 0.01$. Abbreviations: Ctrl, control; DAPI, 4′,6-diamidino-2-phenylindole; GFP, green fluorescent protein; IP, immunoprecipitation; n.s., not significant; Veh, vehicle.

HSC-SPECIFIC KNOCKOUT OF Sirt6 EXACERBATES CCl_4-INDUCED AND DDC-INDUCED LIVER FIBROSIS

To test the *in vivo* function of Sirt6 in liver fibrosis, we used two fibrotic models: the CCl_4 causes liver fibrosis by damaging hepatocytes, and DDC induces liver fibrosis because of cholestasis.[24,25] The CCl_4 model is illustrated in Fig. 6B (lower panel). CCl_4 causes significant hepatic fibrosis in $Sirt6^{f/f}$ mice as assessed by Sirius red and Masson staining and the quantification of hydroxyproline (Fig. 6C). As compared with $Sirt6^{f/f}$ mice, $Sirt6^{\triangle HSC}$ mice showed much worse liver fibrosis (Fig. 6C, left panel). Consistently, the level of hydroxyproline was significantly higher in $Sirt6^{\triangle HSC}$ than $Sirt6^{f/f}$ mice (Fig. 6C, right panel). The mRNA expression of fibrotic markers *α-SMA* and collagens was higher in liver of $Sirt6^{\triangle HSC}$ than $Sirt6^{f/f}$ mice after CCl_4 treatment (Fig. 6D,E). The protein levels of α-SMA and Col1a1 were also greatly increased in CCl_4-treated $Sirt6^{\triangle HSC}$ mice (Fig. 6F, left panel). Consistent with the *in vitro* data, the acetylation and phosphorylation of Smad2 was further elevated in the livers of CCl_4-treated $Sirt6^{\triangle HSC}$ mice (Fig. 6F, right panel). The deletion of Sirt6 in HSC appeared to have little effect on CCl_4-induced liver injury because the serum levels of alanine aminotransferase (ALT) and aspartate aminotransferase (AST) were comparable between $Sirt6^{f/f}$ and $Sirt6^{\triangle HSC}$ mice (Supporting Fig. S7A,B).

In another independent model of DDC diet-induced liver fibrosis, the hepatic collagen deposition was higher in $Sirt6^{\triangle HSC}$ than $Sirt6^{f/f}$ mice, as shown by Sirius red and Masson staining and quantification of hydroxyproline (Supporting Fig. S8A-C). DCC-treated $Sirt6^{\triangle HSC}$ mice also showed increased mRNA expression of the fibrotic genes *α-SMA*, collagens, tissue inhibitor of metalloproteinase 1/2 (*Timp-1/2*), and matrix metalloproteinase 9 (*MMP9*) (Supporting Fig. S8D,E) and the protein levels of α-SMA and Col1a1 (Supporting Fig. S8F). The phosphorylation of Smad2 was also higher in the livers of $Sirt6^{\triangle HSC}$ mice (Supporting Fig. S8F). Sirt6 deletion had no effect on DDC-induced liver injury, as indicated by similar serum levels of ALT and AST (Supporting Fig. S9A,B). Therefore, Sirt6 ablation in HSC conferred susceptibility to CCl4-induced and DDC-induced hepatic fibrosis.

PHARMACOLOGICAL ACTIVATION OF Sirt6 ALLEVIATES LIVER FIBROSIS

Next, we explored the therapeutic potential of the Sirt6 agonist MDL-800 for liver fibrosis. Mice were injected with CCl_4 for 4 weeks and then treated with RGD-Lip/MDL-800 (10 mg/kg) once every 3 days (Fig. 7A). To demonstrate the specificity of the drug delivery system *in vivo*, our FACS analysis showed that the fluorescent intensity in HSCs was markedly higher than that in hepatocytes, Kupffer cells, liver sinusoidal endothelial cells (LSECs), and biliary cells from livers of CCl_4 mice treated with RGD-Lip/DiD (Supporting Fig. S10A,B). Immunofluorescence staining also confirmed that RGD-Lip–delivered DiD was localized in α-SMA–positive cells, which were aHSCs (Supporting Fig. S10C). HSC-specific delivery of MDL-800 was further confirmed by liquid chromatography–MS, showing the concentration of ML-800 was more than 9.28 times higher in HSCs than hepatocytes, Kupffer cells, biliary cells, and endothelial cells (Supporting Fig. S10D). Treating wild-type (WT) mice with RGD-Lip/MDL-800 attenuated CCl_4-induced liver fibrosis, as shown by Sirius red and

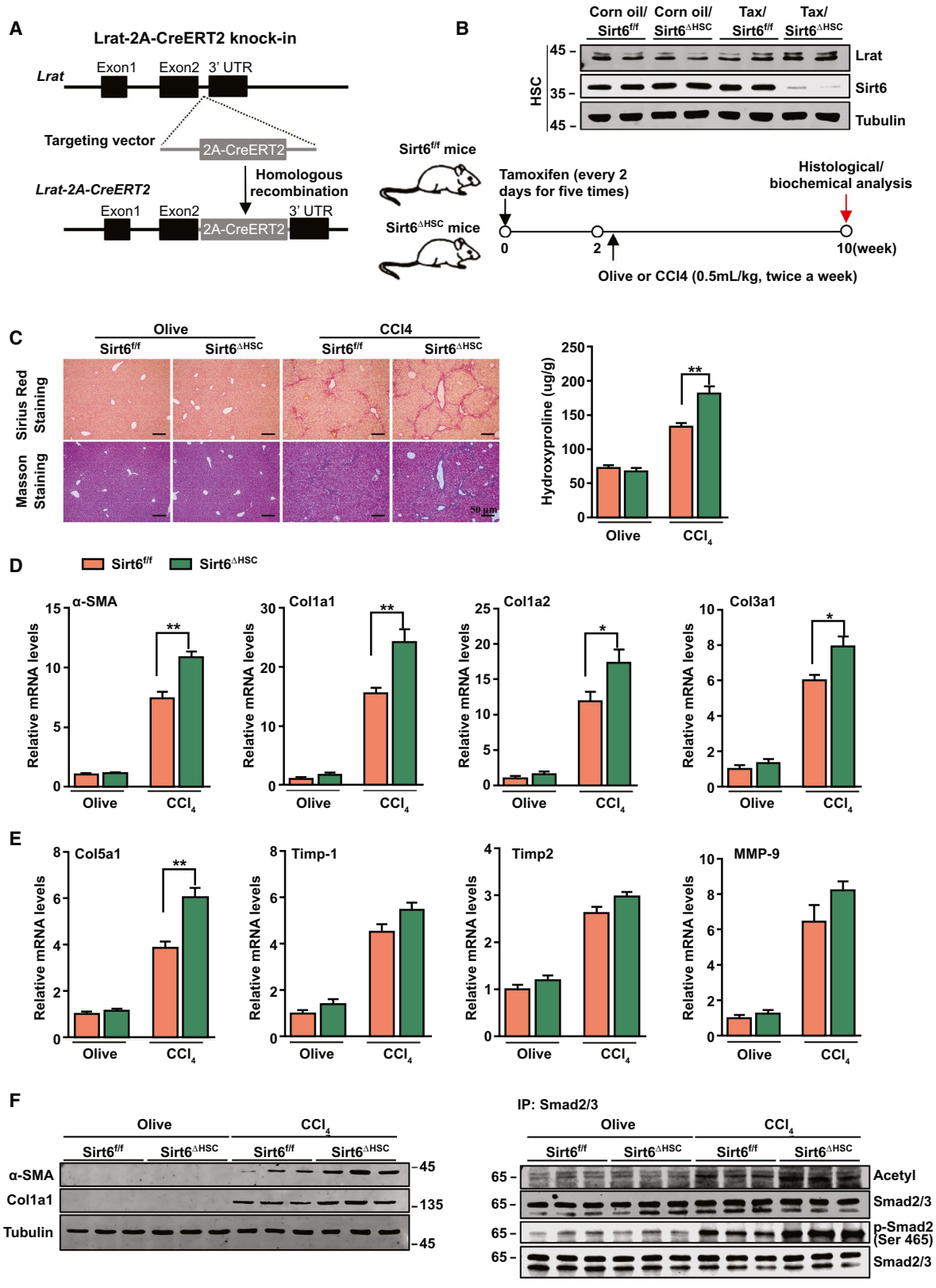
A
Lrat-2A-CreERT2 knock-in
Lrat
Exon1
Exon2
3' UTR
Targeting vector
2A-CreERT2
Lrat-2A-CreERT2
Homologous recombination
Exon1
Exon2
2A-CreERT2
3' UTR
B
Corn oil/ Sirt6f/f
Corn oil/ Sirt6ΔHSC
Tax/ Sirt6f/f
Tax/ Sirt6ΔHSC
HSC
45
35
45
Lrat
Sirt6
Tubulin
Sirt6f/f mice
Sirt6ΔHSC mice
Tamoxifen (every 2 days for five times)
Histological/ biochemical analysis
0
2
10(week)
Olive or CCl4 (0.5mL/kg, twice a week)
C
Olive
CCl4
Sirt6f/f
Sirt6ΔHSC
Sirius Red Staining
Masson Staining
50 μm
Hydroxyproline (ug/g)
Olive
CCl4
D
Sirt6f/f
Sirt6ΔHSC
α-SMA
Col1a1
Col1a2
Col3a1
Relative mRNA levels
Olive
CCl4
E
Col5a1
Timp-1
Timp2
MMP-9
Relative mRNA levels
Olive
CCl4
F
Olive
CCl4
Sirt6f/f
Sirt6ΔHSC
α-SMA
Col1a1
Tubulin
45
135
45
IP: Smad2/3
Acetyl
Smad2/3
p-Smad2 (Ser 465)
Smad2/3

FIG. 6. HSC-specific ablation of Sirt6-exacerbated CCl4-induced liver fibrosis. (A) Schematic showing the strategy for generating the Lrat-2A-CreERT2 knock-in line by homologous recombination. (B) Upper panel: western blot analysis of the deletion of Sirt6 in HSCs. Lower panel: regimen of $Sirt6^{f/f}$ and $Sirt6^{\Delta HSC}$ mice receiving olive oil or CCl_4 (0.5 mL/kg) for 8 weeks after tamoxifen-induced deletion of Sirt6. (C) Left panel: fibrosis assessed by Sirius red and Masson staining. Right panel: quantification of hepatic hydroxyproline. (D,E) Real-time quantitative PCR analysis of mRNA levels of fibrotic genes in livers of 4 groups. (F) Western blot analysis of protein levels of α-SMA, Col1a1, acetyl, phosphorylated (p-)Smad2 (Ser465), and Smad2/3. Data are mean ± SEM. n = 7. $^*P < 0.05$, $^{**}P < 0.01$. Abbreviations: Col5a1, collagen type V alpha 1 chain; IP, immunoprecipitation; Tax, tamoxifen; UTR, untranslated region.

Masson staining and quantification of hydroxyproline (Fig. 7B-C). The induction of fibrotic genes such as *α-SMA*, collagens, *Timp1/2*, and *MMP9* was also decreased (Fig. 7D,E). Western blot analysis confirmed the reduced protein levels of Col1a1 and α-SMA (Fig. 7F, left panel). Consistently, activation of Sirt6 suppressed the acetylation and phosphorylation level of Smad2 (Fig. 7F, right panel). Sirt6 agonist did not alleviate liver injury induced by CCl_4, as shown by similar serum ALT and AST levels (Supporting Fig. S11A,B).

Treating WT mice with RGD-Lip/MDL-800 also alleviated DDC-induced liver fibrosis (Supporting Fig. S12A-C). The DDC-responsive expression of fibrotic genes was suppressed in RGD-Lip/MDL-800–treated mice (Supporting Fig. S12D,E). The protein levels of Col1a1, α-SMA, and phosphorylated Smad2 were also decreased (Supporting Fig. S12F). Again, the activation of Sirt6 had little effect on liver injury (Supporting Fig. S13A,B).

Discussion

Liver fibrosis can be a common outcome of different chronic liver injuries, and HSCs play a central role in its development.[4,26,27] In the present study, Sirt6 was most abundantly expressed in HSCs compared with other liver cell types, and Sirt6 expression was decreased during the activation of HSCs. By using both loss-of-function and gain-of-function models, we revealed that Sirt6 plays a key role in HSC activation. Mechanistically, Sirt6 inhibited TGF-β signaling by antagonizing Smad2 activity. Sirt6 physically interacted with Smad2 and regulated its acetylation level. MS revealed that lysine 54 in Smad2 was deacetylated by Sirt6. Mutation of lysine 54 to Arginine in Smad2 decreased the acetylation of Smad2 and lowered its transcriptional activity. More importantly, mutation of Smad2 on lysine 54 abolished the regulatory effect of Sirt6 on Smad2 transcriptional activity. *In vivo* results showed that HSC-specific deletion of Sirt6 exacerbated CCl_4-induced and DDC-induced liver fibrosis. Pharmacological activation of Sirt6 by targeted delivery of a Sirt6 agonist into HSCs protected mice against CCl_4-induced and DDC-induced liver fibrosis.

The TGF-β signaling pathway has been established as an important profibrogenic factor that induces the transdifferentiation of HSCs to myofibroblasts and ECM accumulation.[7,28,29] TGF-β binds to its receptor, causes phosphorylation of Smad2/3, and triggers transcription of downstream factors. Recent studies revealed that acetylation of Smad2/3 also plays an important role in this pathway.[9,30,31] Smad2/3 can interact with the transcriptional coactivators p300/CBP. p300/CBP could acetylate Smad2 and resulted in enhanced Smad-mediated transcription.[9,21,32,33] A major acetylation site of Smad2 by p300/CBP is Lysine 378 in the MH2 domain known to be critical for regulating transcriptional activity.[34] For Smad2, lysine 19, lysine 20, and lysine 39 are also required for efficient acetylation, and the acetylation of these lysines is required for the ability of Smad2 to mediate activin and TGF-β signaling.[10] In this study, MS revealed an acetylation of Smad2. Although both Smad2 and Smad3 are the major downstream mediators of TGF-β signaling, our MS analysis found that Sirt6 only regulated the acetylation of Smad2, but it had little effect on the acetylation of Smad3. Future studies are necessary to understand the differential targeting of Smad2 by Sirt6.

Lysine 54 on Smad2 resides in the MH1 domain, which was thought to be the major acetylation domain in Smad2.[11] Mutation of lysine 54 to arginine greatly decreased TGF-β–induced acetylation of Smad2. The acetylation of lysine 54 appeared to be required for the phosphorylation and nuclear translocation of Smad2. Mutation of lysine 54 abolished the regulatory effect of Sirt6 on the acetylation, phosphorylation, nuclear localization, and transcriptional activity of Smad2. The relationship between acetylation and

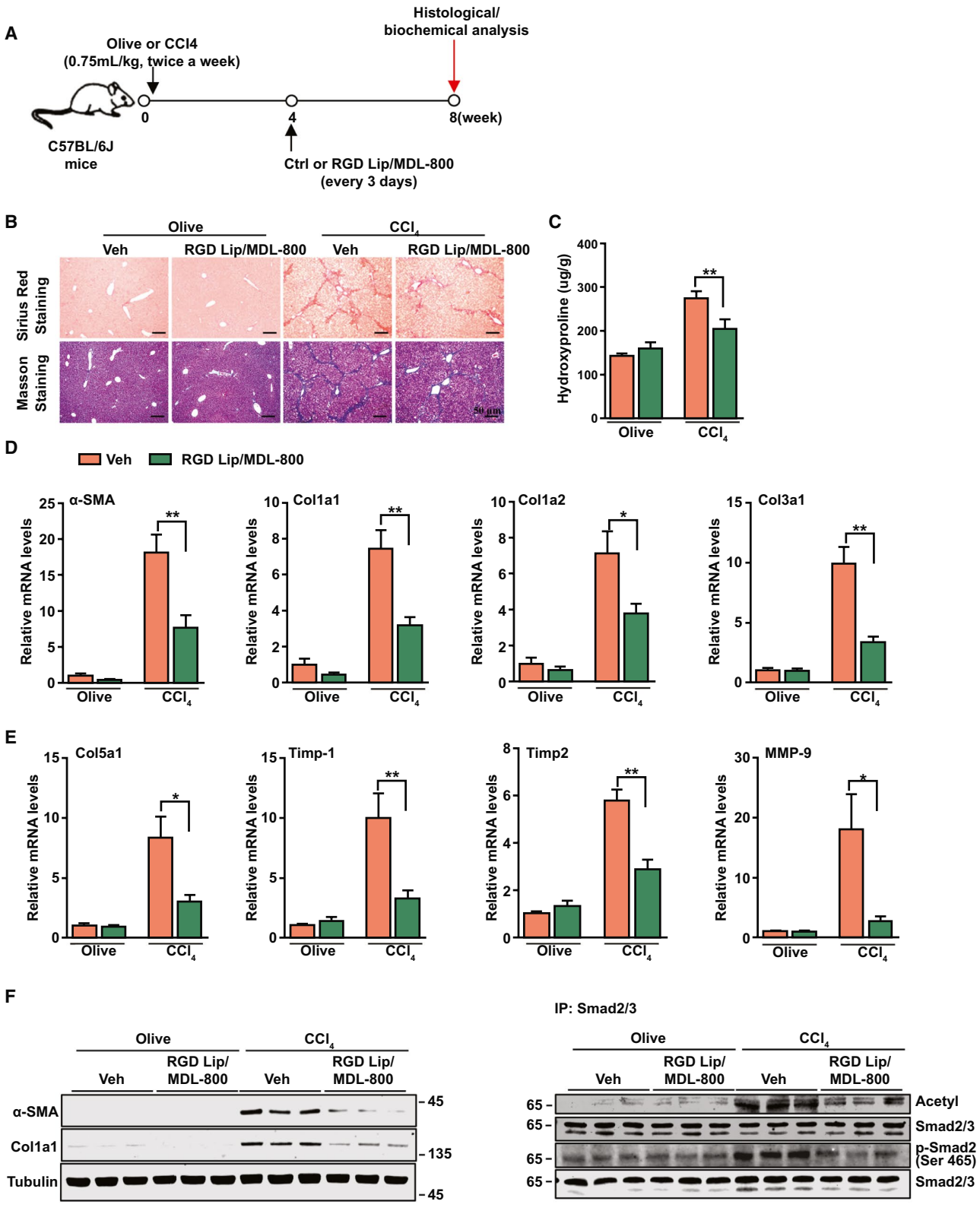
A
Olive or CCl4
(0.75mL/kg, twice a week)
Histological/
biochemical analysis
0
4
8(week)
C57BL/6J
mice
Ctrl or RGD Lip/MDL-800
(every 3 days)
B
Olive
CCl4
Veh
RGD Lip/MDL-800
Veh
RGD Lip/MDL-800
Sirius Red
Staining
Masson
Staining
50 μm
C
Hydroxyproline (ug/g)
400
300
200
100
0
**
Olive
CCl4
D
Veh
RGD Lip/MDL-800
α-SMA
Col1a1
Col1a2
Col3a1
Relative mRNA levels
Olive
CCl4
E
Col5a1
Timp-1
Timp2
MMP-9
F
IP: Smad2/3
Olive
CCl4
Veh
RGD Lip/
MDL-800
α-SMA
Col1a1
Tubulin
45
135
45
65
Acetyl
Smad2/3
p-Smad2
(Ser 465)
Smad2/3

FIG. 7. Target delivery of Sirt6 agonist, MDL-800, to HSCs protected against CCl_4-induced liver fibrosis. (A) The regimen of targeted delivery of Sirt6 agonist MDL-800. WT mice were treated with olive oil or CCl_4 (0.75 mL/kg) for 8 weeks. During the last 4 weeks, mice were given RGD-Lip or RGD-Lip/MDL-800 (10 mg/kg) every 3 days by tail-vein injection. (B) Fibrosis was assessed by Sirius red and Masson staining. (C) Level of hepatic hydroxyproline. (D,E) Real-time quantitative PCR analysis of mRNA levels of fibrotic genes in liver. (F) Western blot analysis of protein levels of α-SMA, Col1a1, acetyl, phosphorylated (p-)Smad2 (Ser465), and Smad2/3. Data are mean ± SEM. n = 7. $^*P < 0.05$, $^{**}P < 0.01$. Abbreviations: Col5a1, collagen type V alpha 1 chain; Ctrl, control; IP, immunoprecipitation; Veh, vehicle.

phosphorylation has been reported in several previous studies. p53 phosphorylation of Ser46 leads to the acetylation of Lys382, which is necessary for p53-mediated apoptosis.[35] Our study found that mutation of lysine 54 on Smad2 decreased the phosphorylation level, thereby confirming that Smad2 acetylation can affect its phosphorylation.

Studies used collagen-driven Cre, desmin-Cre, human glial fibrillary acidic protein (hGFAP)-Cre, and glial fibrillar acidic protein (GFAP)-Cre to track HSCs and study the function of different genes in liver fibrosis.[36] However, these Cre lines failed to specifically label HSCs.[23,36] Lrat-Cre transgenic mice were confirmed to specifically label HSCs and have been used to study the HSC function of genes.[23,37] However, this Lrat-Cre transgenic mouse line can only pass the Cre transgene to female descendants,[23] and the expression of Cre is constitutive, which limits its utility. In this study, we generated a tamoxifen-inducible CreERT2 mouse line by knocking in the CreERT2 right after exon 2 of *Lrat* connected by 2A. Characterization of the Lrat-CreERT2 mouse line showed that CreERT2 was specifically expressed in HSCs but not in other liver cell types. When crossed with $Sirt6^{f/f}$ mice, HSC-specific Sirt6-deficient mice ($Sirt6^{\triangle HSC}$) were created. $Sirt6^{\triangle HSC}$ mice showed specific deletion of Sirt6 in HSCs under the control of tamoxifen. Therefore, the Lrat-CreERT2 mouse line allows for cell type–specific and spatial-specific deletion of genes in HSCs for a powerful tool in the field of HSC study.

MDL-800 was reported as a selective agonist of Sirt6.[19] MDL-800 activates Sirt6 by increasing the binding affinities of acetylated substrates and cofactors as well as increasing the catalytic efficiency of Sirt6.[19] However, systemic MDL-800 treatment may cause side effects and potential toxicity. To overcome these problems, we loaded MDL-800 into RGD-guided Lip (RGD-Lip/MDL-800). RGD is a pentapeptide that binds with high affinity to integrin αV and β3, which are highly expressed in aHSCs. We showed that RGD-Lip can specifically target aHSCs *in vivo*.[20,38] Indeed, we found that RGD-Lip–delivered MDL-800 showed a 10.5-fold higher concentration of MDL-800 in HSCs than in other liver cell types isolated from the same mice. Moreover, targeted delivery of MDL-800 to HSCs decreased Smad2 phosphorylation and protected mice against CCl_4-induced and DDC diet-induced liver fibrosis (Fig. 7 and Supporting Fig. S9). Targeted delivery of MDL-800 to activate Sirt6 in HSCs by RGD-Lip may be a promising treatment to manage liver fibrosis.

Sirt6 has been reported as an inhibitor of cardiac fibroblast differentiation and a negative regulator of angiotensin II–mediated myocardial remodeling, fibrosis, and injury.[39,40] In kidney fibrosis and other diseases, Sirt6 protects against fibrosis and injury by epigenetic regulation of histones in proximal tubules or podocytes.[16,41,42] Sirt6 also acts as a key modulator in the epithelial to mesenchymal transition by inactivating TGF-β1 and nuclear factor-κB signaling pathways, which suggests that Sirt6 may be an attractive therapeutic target for idiopathic pulmonary fibrosis.[43,44] Although reports suggested that Sirt6 may play a role in liver fibrosis,[13,15,17,45] whether the liver fibrosis observed in Sirt6-null mice was a direct or indirect result of Sirt6 ablation was unclear. The cell type responsible for liver fibrosis in Sirt6 null mice was also not clear. By using HSC-specific Sirt6-knockout mice, we demonstrated a direct role of Sirt6 in HSC activation and liver fibrosis. Although our study demonstrated that the Sirt6 in HSCs plays an important role in liver fibrosis, the contribution of Sirt6 in hepatocytes to liver fibrosis should not be ignored. Several studies showed that Sirt6 in hepatocytes protected against hepatic steatosis, insulin resistance, and inflammation.[17,46-48] Because steatosis and inflammation are risk factors for HSC activation and liver fibrosis, it is possible that Sirt6 in hepatocytes may also participate in the initiation or progression of liver fibrosis.

In summary, we have established Sirt6 as an anti-fibrogenic factor in HSC activation and liver fibrosis.

Sirt6 agonists and strategies that preferentially activate Sirt6 in HSCs may represent approaches to prevent and treat liver fibrosis.

Author Contributions: Jinhang Zhang, Y.L., and J.H. designed the experiments; Jinhang Zhang and Y.L. performed experiments. Q.L., Y.H., R.L., T.W., Z.Z., Jian Zhou, H.H., Q.T., C.H., Y.Z., and G.Z. helped with experiments. W.J., W.X., and L.M. contributed to the discussion and reviewed the manuscript. Jian Zhang provided the Sirt6 agonist ML-800. Jinhang Zhang and J.H. wrote the manuscript. J.H. obtained funding. Jinhang Zhang and J.H. are the guarantors of this work and, as such, had full access to all the data in the study and take responsibility for the integrity of the data and the accuracy of the data analysis.

REFERENCES

1) Bataller R, Brenner DA. Liver fibrosis. J Clin Invest 2005;115: 209-218.
2) Friedman SL. Liver fibrosis—from bench to bedside. J Hepatol 2003;38:38-53.
3) Sun M, Kisseleva T. Reversibility of liver fibrosis. Clin Res Hepatol Gastroenterol 2015;39(Suppl. 1):S60-S63.
4) Higashi T, Friedman SL, Hoshida Y. Hepatic stellate cells as key target in liver fibrosis. Adv Drug Deliv Rev 2017;121:27-42.
5) Tsuchida T, Friedman SL. Mechanisms of hepatic stellate cell activation. Nat Rev Gastroenterol Hepatol 2017;14:397-411.
6) Friedman SL. Hepatic stellate cells: protean, multifunctional, and enigmatic cells of the liver. Physiol Rev 2008;88:125-172.
7) Caja L, Dituri F, Mancarella S, Caballero-Diaz D, Moustakas A, Gianelli G, et al. TGF-beta and the tissue microenvironment: relevance in fibrosis and cancer. Int J Mol Sci 2018;19:1294.
8) Axel M, Gressner RW, Breitkopf K, Dooluy S. Roles of TGF-beta in hepatic fibrosis. Front Biosci 2002;7:d793-d807.
9) Wrighton KH, Feng XH. To (TGF)beta or not to (TGF)beta: fine-tuning of Smad signaling via post-translational modifications. Cell Signal 2008;20:1579-1591.
10) Tu AW, Luo K. Acetylation of Smad2 by the co-activator p300 regulates activin and transforming growth factor beta response. J Biol Chem 2007;282:21187-21196.
11) Simonsson M, Kanduri M, Grönroos E, Heldin C-H, Ericsson J. The DNA binding activities of Smad2 and Smad3 are regulated by coactivator-mediated acetylation. J Biol Chem 2006;281:39870-39880.
12) Tasselli L, Zheng W, Chua KF. SIRT6: novel mechanisms and links to aging and disease. Trends Endocrinol Metab 2017;28:168-185.
13) Mostoslavsky R, Chua KF, Lombard DB, Pang WW, Fischer MR, Gellon L, et al. Genomic instability and aging-like phenotype in the absence of mammalian SIRT6. Cell 2006;124:315-329.
14) Kanfi Y, Naiman S, Amir G, Peshti V, Zinman G, Nahum L, et al. The sirtuin SIRT6 regulates lifespan in male mice. Nature 2012;483:218-221.
15) **Xiao C**, **Wang RH**, **Lahusen TJ**, Park O, Bertola A, Maruyama T, et al. Progression of chronic liver inflammation and fibrosis driven by activation of c-JUN signaling in Sirt6 mutant mice. J Biol Chem 2012;287:41903-41913.
16) Muraoka H, Hasegawa K, Sakamaki Y, Minakuchi H, Kawaguchi T, Yasuda I, et al. Role of Nampt-Sirt6 axis in renal proximal tubules in extracellular matrix deposition in diabetic nephropathy. Cell Rep 2019;27:199-212.e5.
17) Ka SO, Bang IH, Bae EJ, Park BH. Hepatocyte-specific sirtuin 6 deletion predisposes to nonalcoholic steatohepatitis by up-regulation of Bach1, an Nrf2 repressor. FASEB J 2017;31:3999-4010.
18) Mederacke I, Dapito DH, Affò S, Uchinami H, Schwabe RF. High-yield and high-purity isolation of hepatic stellate cells from normal and fibrotic mouse livers. Nat Protoc 2015;10:305-315.
19) Huang Z, Zhao J, Deng W, Chen Y, Shang J, Song K, et al. Identification of a cellularly active SIRT6 allosteric activator. Nat Chem Biol 2018;14:1118-1126.
20) **Li Y**, **Pu S**, Liu Q, Li R, Zhang J, Wu T, et al. An integrin-based nanoparticle that targets activated hepatic stellate cells and alleviates liver fibrosis. J Control Release 2019;303:77-90.
21) Wang Y, Tu K, Liu D, Guo L, Chen Y, Li Q, et al. p300 acetyltransferase is a cytoplasm-to-nucleus shuttle for SMAD2/3 and TAZ nuclear transport in transforming growth factor beta-stimulated hepatic stellate cells. Hepatology 2019;70:1409-1423.
22) García-Vizcaíno EM, Liarte S, Alonso-Romero JL, Nicolás FJ. Sirt1 interaction with active Smad2 modulates transforming growth factor-beta regulated transcription. Cell Commun Signal 2017;15:50.
23) Mederacke I, Hsu CC, Troeger JS, Huebener P, Mu X, Dapito DH, et al. Fate tracing reveals hepatic stellate cells as dominant contributors to liver fibrosis independent of its aetiology. Nat Commun 2013;4:2823.
24) Fickert P, Stöger U, Fuchsbichler A, Moustafa T, Marschall HU, Weiglein AH, et al. A new xenobiotic-induced mouse model of sclerosing cholangitis and biliary fibrosis. Am J Pathol 2007;171:525-536.
25) Valeria Mariottia MS, Fabrisa L, Calvisi DF. Animal models of biliary injury and altered bile acid metabolism. Biochim Biophys Acta Mol Basis Dis 2018;1864:1254-1261.
26) Mehta KJ, Farnaud SJ, Sharp PA. Iron and liver fibrosis: mechanistic and clinical aspects. World J Gastroenterol 2019;25: 521-538.
27) **Gutiérrez-Grobe Y**, **Juárez-Hernández E**, Sánchez-Jiménez BA, Uribe-Ramos MH, Ramos-Ostos MH, Uribe M, et al. Less liver fibrosis in metabolically healthy compared with metabolically unhealthy obese patients with non-alcoholic fatty liver disease. Diabetes Metab 2017;43:332-337.
28) Zehender A, Huang J, Györfi AH, Matei AE, Trinh-Minh T, Xu X, et al. The tyrosine phosphatase SHP2 controls TGFβ-induced STAT3 signaling to regulate fibroblast activation and fibrosis. Nat Commun 2018;9:3259.
29) Herrera B, Addante A, Sanchez A. BMP signalling at the crossroad of liver fibrosis and regeneration. Int J Mol Sci 2017;19:39.
30) Kim S, Lim JH, Woo CH. ERK5 inhibition ameliorates pulmonary fibrosis via regulating Smad3 acetylation. Am J Pathol 2013;183:1758-1768.
31) Bugyei-Twum A, Ford C, Civitarese R, Seegobin J, Advani SL, Desjardins JF, et al. Sirtuin 1 activation attenuates cardiac fibrosis in a rodent pressure overload model by modifying Smad2/3 transactivation. Cardiovasc Res 2018;114:1629-1641.
32) **Shen X**, **Hu PP**, **Liberati NT**, Datto MB, Frederick JP, Wang XF. TGF-beta–induced phosphorylation of Smad3 regulates its interaction with coactivator p300/CREB-binding protein. Mol Biol Cell 1998;9:3309-3319.
33) Ralf Janknecht NJW, Hunter T. TGF-beta-stimulated cooperation of Smad proteins with the coactivators CBP/p300. Genes Dev 1998;12:2114-2119.

34) Inoue Y, Itoh Y, Abe K, Okamoto T, Daitoku H, Fukamizu A, et al. Smad3 is acetylated by p300/CBP to regulate its transactivation activity. Oncogene 2007;26:500-508.
35) Hofmann TG, Möller A, Sirma H, Zentgraf H, Taya Y, Dröge W, et al. Regulation of p53 activity by its interaction with homeodomain-interacting protein kinase-2. Nat Cell Biol 2002;4:1-10.
36) Kinoshita K, Iimuro Y, Fujimoto J, Inagaki Y, Namikawa K, Kiyama H, et al. Targeted and regulable expression of transgenes in hepatic stellate cells and myofibroblasts in culture and in vivo using an adenoviral Cre/loxP system to antagonise hepatic fibrosis. Gut 2007;56:396-404.
37) Yan J, Tung HC, Li S, Niu Y, Garbacz WG, Lu P, et al. Aryl hydrocarbon receptor signaling prevents activation of hepatic stellate cells and liver fibrogenesis in mice. Gastroenterology 2019;157:793-806.
38) **Li F**, **Song Z**, Li Q, Wu J, Wang J, Xie C, et al. Molecular imaging of hepatic stellate cell activity by visualization of hepatic integrin alphavbeta3 expression with SPECT in rat. Hepatology 2011;54:1020-1030.
39) Tian K, Liu Z, Wang J, Xu S, You T, Liu P. Sirtuin-6 inhibits cardiac fibroblasts differentiation into myofibroblasts via inactivation of nuclear factor kappaB signaling. Transl Res 2015;165:374-386.
40) **Zhang ZZ**, **Cheng YW**, **Jin HY**, **Chang Q**, Shang QH, Xu YL, et al. The sirtuin 6 prevents angiotensin II-mediated myocardial fibrosis and injury by targeting AMPK-ACE2 signaling. Oncotarget 2017;8:72302-72314.
41) Cai J, Liu Z, Huang X, Shu S, Hu X, Zheng M, et al. The deacetylase sirtuin 6 protects against kidney fibrosis by epigenetically blocking β-catenin target gene expression. Kidney Int 2019;97:106-118.
42) Liu M, Liang K, Zhen J, Zhou M, Wang X, Wang Z, et al. Sirt6 deficiency exacerbates podocyte injury and proteinuria through targeting Notch signaling. Nat Commun 2017;8:413.
43) Tian K, Chen P, Liu Z, Si S, Zhang Q, Mou Y, et al. Sirtuin 6 inhibits epithelial to mesenchymal transition during idiopathic pulmonary fibrosis via inactivating TGF-β1/Smad3 signaling. Oncotarget 2017;8:61011-61024.
44) Zhang Q, Tu W, Tian K, Han L, Wang Q, Chen P, et al. Sirtuin 6 inhibits myofibroblast differentiation via inactivating transforming growth factor-β1/Smad2 and nuclear factor-κB signaling pathways in human fetal lung fibroblasts. J Cell Biochem 2019;120:93-104.
45) **Maity S**, **Muhamed J**, Sarikhani M, Kumar S, Ahamed F, Mrudula Spurthi K, et al. Sirtuin 6 deficiency transcriptionally up-regulates TGF-β signaling and induces fibrosis in mice. J Biol Chem 2020;295:415-434.
46) **Luo P**, **Qin C**, **Zhu L**, Fang C, Zhang Y, Zhang H, et al. Ubiquitin-specific peptidase 10 (USP10) inhibits hepatic steatosis, insulin resistance, and inflammation through Sirt6. Hepatology 2018;68:1786-1803.
47) Kim HG, Huang M, Xin Y, Zhang Y, Zhang X, Wang G, et al. The epigenetic regulator SIRT6 protects the liver from alcohol-induced tissue injury by reducing oxidative stress in mice. J Hepatol 2019;71:960-969.
48) Bang IH, Kwon OK, Hao L, Park D, Chung MJ, Oh BC, et al. Deacetylation of XBP1s by sirtuin 6 confers resistance to ER stress-induced hepatic steatosis. Exp Mol Med 2019;51:1-11.

Author names in bold designate shared co-first authorship.

Supporting Information

Additional Supporting Information may be found at onlinelibrary.wiley.com/doi/10.1002/hep.31418/suppinfo.